ESANN'1997 proceedings - European Symposium on Artificial Neural Networks
Bruges (Belgium), 16-17-18 April 1997, D-Facto public., ISBN 2-9600049-7-3, pp. 67-72

# Neural Network for Color Contrast Gain Control

Michael D'Zmura

Department of Cognitive Sciences
University of California, Irvine
Irvine, California 92697 USA
mdzmura@uci.edu

**Abstract.** I present a model for visual contrast gain control that is based on results from psychophysical experiments on human vision. The model pools contrast in channels that are tuned for spatial frequency, orientation and color and combines these contrasts selectively to determine channel gain. The chief effect of the contrast gain control is to equalize contrast levels across space. Characteristic images for the model show that the contrast gain control also equalizes contrast across spatial frequency and orientation. The receptive field of a model neuron comprises a standard, linear receptive field and a large inhibitory surround provided by the contrast gain control. This processing accounts for a variety of psychophysical results on contrast induction and for many visual illusions produced by contrast-modulated stimuli.

## 1. Introduction

Electrophysiological work by Shapley and Victor (1979) initiated a number of investigations of the response gain of neurons in the retino-cortical pathways during the 1980s. Heeger (1992) proposed an influential model for the results, in which neurons are tuned to varying spatial frequency and orientation and have their own contrast gain control that acts through divisive normalization. Such a normalization helps to match neuronal channel capacity to the visual signal, and to provide for contrast constancy under changing conditions of viewing, for instance, to compensate for fog or haze (Robson 1988). Sperling (1989) proposed a psychophysical model of human spatial vision with a contrast gain control, and work on contrast induction by Chubb, Sperling and Solomon (1989) drew a direct parallel between physiological contrast gain control and the perceptual phenomenon of contrast induction, which is demonstrated in Figure 1. The two disks, at left and right, have physically identical contrasts. Yet most observers agree that the disk on the right has a higher apparent contrast than the disk on the left: the white is whiter and the black is blacker. One infers that the visual system has an automatic contrast gain control: in response to the high contrast of the annulus at left, the visual system reduces contrast gain, while in response to the low contrast of the area that surrounds the disk at right, it increases contrast gain. The result is the apparent difference in disk contrast. In my own work with contrast induction, performed in collaboration with B. Singer, the initial questions were whether contrast induction was a feature of color vision and whether

ESANN'1997 proceedings - European Symposium on Artificial Neural Networks
Bruges (Belgium), 16-17-18 April 1997, D-Facto public., ISBN 2-9600049-7-3, pp. 67-72

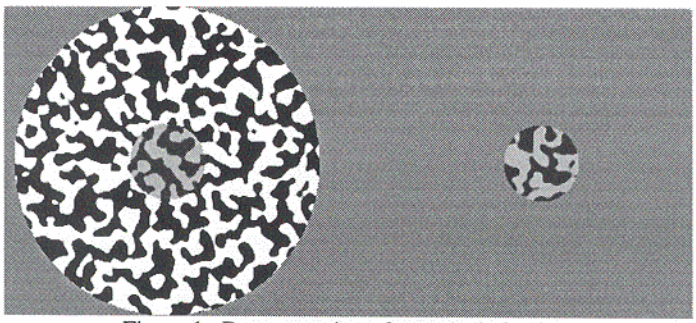

Figure 1. Demonstration of contrast induction.

there existed contrast gain controls within color-sensitive pathways. We created colored, isoluminant versions of Figure 1 and observed variations in apparent color contrast, similar to those shown with the achromatic stimuli. We continued with experiments to characterize the mechanisms responsible for the contrast induction, and turned to the work on contrast gain control to help provide physiological underpinnings (Singer and D'Zmura 1994; Singer and D'Zmura 1995; D'Zmura and Singer 1996; D'Zmura in press). The resulting model is presented here.

## 2. Multiresolution Model

Model channels are selective for color, spatial frequency and orientation. Each channel response is multiplied by a gain that depends on the local contrasts of the channels. These local contrasts depend on channel response and on contrast pooling functions with sizes that depend on channel spatial frequency. We used four octave-wide spatial frequency sensitivities, six orientation sensitivities of width 30 deg, and three chromatic sensitivities (A, L&M and S) to create the model. These chromatic sensitivities correspond to the three basic axes in the color space of Derrington, Krauskopf and Lennie (1984): an achromatic intensity axis (A), a red-green axis (L&M) and a yellow-blue axis (S). The spatial frequency sensitivities of the channels are described by non-overlapping regions of the spatial frequency plane (see Fig. 2). Spatial frequency, orientation and color sensitivities were combined factorially to produce 72 channels.

Model computation starts with a color decomposition of an input image into achromatic, L&M-cone axis and S-cone axis components. These three color components $r_A$, $r_{LM}$ and $r_S$ are determined by appropriate linear combinations of an input image's RGB values, after the image has been stripped of its average value:

$$r_i(\mathbf{x}) = a_{i,R}\,(R(\mathbf{x})-R_{avg}) + a_{i,G}\,(G(\mathbf{x})-G_{avg}) + a_{i,B}\,(B(\mathbf{x})-B_{avg}), \qquad (1)$$

for mechanisms i = A, L&M and S. The model then determines the responses of the channels tuned to spatial frequency and orientation by transforming the color responses into the spatial frequency domain and parcelling up the input image among the various channels. Suppose that the functions $G_j(\omega)$, for j = 1,2,3,4, describe the four spatial frequency sensitivities and that the functions $H_k(\phi)$, for k=1,...,6, describe the six orientation sensitivities (as in Fig. 2). The response $r_{ijk}(\mathbf{x})$ of the channel with the $i^{th}$ color, $j^{th}$ spatial frequency and $k^{th}$ orientation sensitivities is then given by:

$$r_{ijk}(\mathbf{x}) = \mathcal{F}^{-1}\,[\,\mathcal{F}\,[\,r_i(\mathbf{x})\,]\,\times\,G_j(\omega)\,\times\,H_k(\phi)\,]\,, \qquad (2)$$

ESANN'1997 proceedings - European Symposium on Artificial Neural Networks
Bruges (Belgium), 16-17-18 April 1997, D-Facto public., ISBN 2-9600049-7-3, pp. 67-72

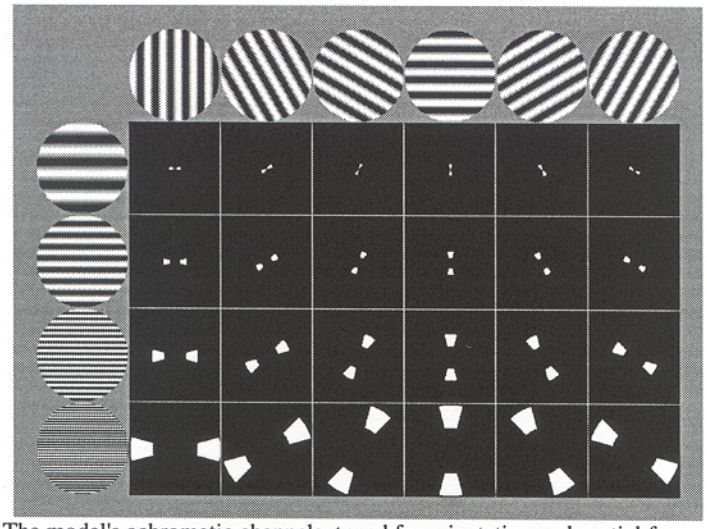

Figure 2. The model's achromatic channels, tuned for orientation and spatial frequency. Each of the 24 plots of channel sensitivity is labeled by a sinusoid in the left column that indicates channel peak spatial frequency and by a sinusoid in the top row that indicates the central orientation of the channel. Each of the 24 sensitivity plots has its origin (frequency 0) in the center; frequency increases as one moves from center to edge. White areas indicate sensitivity.

for i=A, LM, S, j=1,...,4, and k=1,...,6. The original chromatic response $r_i(\mathbf{x})$ to an input image (Eqn. 1) is subject to a Fourier transform $\mathcal{F}$ and is then filtered using $G_j$ and $H_k$ to produce the appropriate response in the spatial frequency domain, which is then transformed back to the space domain to provide the desired response $r_{ijk}(\mathbf{x})$. Figure 3 illustrates the responses of the 24 achromatic channels of the model to a (color) image of a space shuttle vehicle.

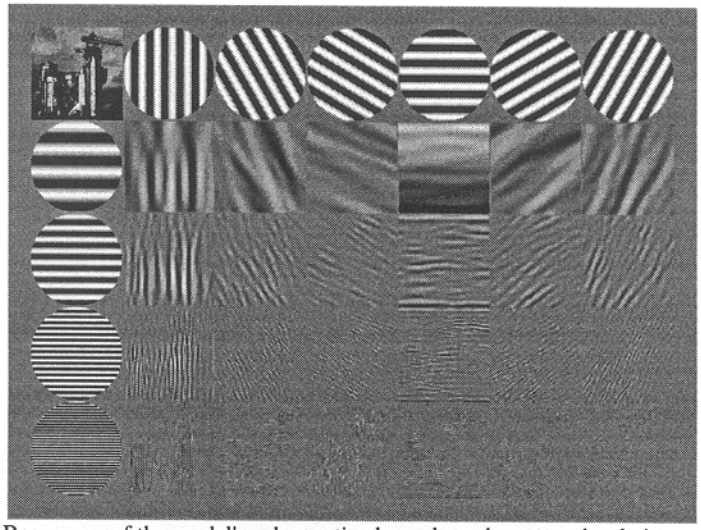

Figure 3. Responses of the model's achromatic channels to the space shuttle image. Brighter values indicate greater responses.

ESANN'1997 proceedings - European Symposium on Artificial Neural Networks
Bruges (Belgium), 16-17-18 April 1997, D-Facto public., ISBN 2-9600049-7-3, pp. 67-72

The model multiplies each of the 72 channel responses at each position by channel-specific gains, which are determined by taking linear combinations of local contrasts found within each of the channels. The local contrast within a channel is computed by taking the absolute value of the channel's response and convolving the result with a Gaussian contrast pooling function of appropriate size. The formula for computing the local contrast $c_{ijk}(\mathbf{x})$ within the ijk$^{th}$ channel, as a function of spatial position, is:

$$c_{ijk}(\mathbf{x}) = N_j(\mathbf{x}) * |r_{ijk}(\mathbf{x})| , \qquad (3)$$

for i=A, LM, and S, j=1,...,4, and k=1,...,6. The Gaussian functions $N_j$ are spatially isotropic and have standard deviations $\sigma_j$ that increase linearly with channel peak wavelength (D'Zmura and Singer 1996). In Figure 4 are shown the local contrasts found within the model's 24 achromatic channels in response to the input image.

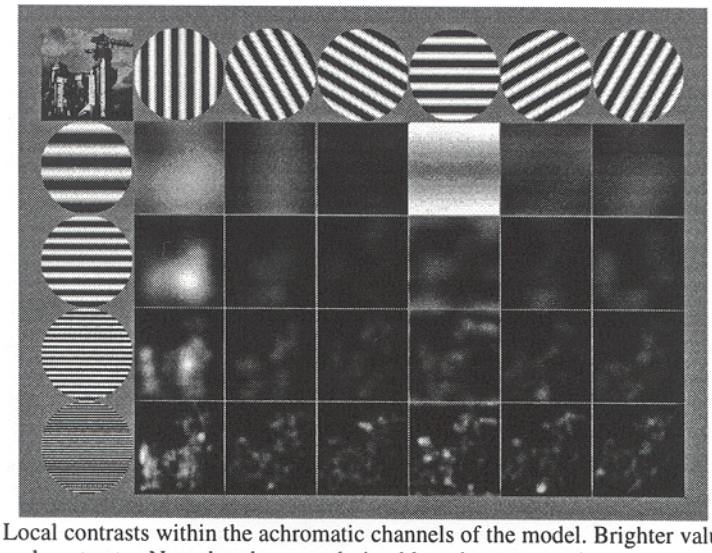

Figure 4. Local contrasts within the achromatic channels of the model. Brighter values indicate higher local contrasts. Note that the convolution blurs the response increasingly as channel peak wavelength increases. Inspection of the local contrast in the low-frequency, horizontally-oriented channel shows that the gradient between sky and ground (see also Fig. 3) has been rectified in the contrast computation.

The gain control forms, for each channel, an appropriate linear combination of the contrast responses which it then uses to inhibit channel signals. The coefficients b that describe channel interaction are set to (negative) values that incorporate psychophysical results on selectivity in spatial frequency, orientation and color (Chubb, Sperling and Solomon 1989; Solomon, Sperling and Chubb 1993; Singer and D'Zmura 1994). Weighted contrasts are summed within each channel's contrast gain control. The gain $g_{ijk}(\mathbf{x})$ on the ijk$^{th}$ channel as a function of spatial position is:

$$g_{ijk}(\mathbf{x}) = g_{ijk} + \sum_{a=A,LM,S} \sum_{b=1}^{4} \sum_{c=1}^{6} b_{ijk,abc}\, c_{abc}(\mathbf{x}) , \qquad (4)$$

for i=A, LM, and S, j=1,...,4, and k=1,...,6. The gain on the ijk$^{th}$ channel depends on the local contrasts in all other channels. Figure 5 shows the gains to be applied to channel responses in our example.

ESANN'1997 proceedings - European Symposium on Artificial Neural Networks
Bruges (Belgium), 16-17-18 April 1997, D-Facto public., ISBN 2-9600049-7-3, pp. 67-72

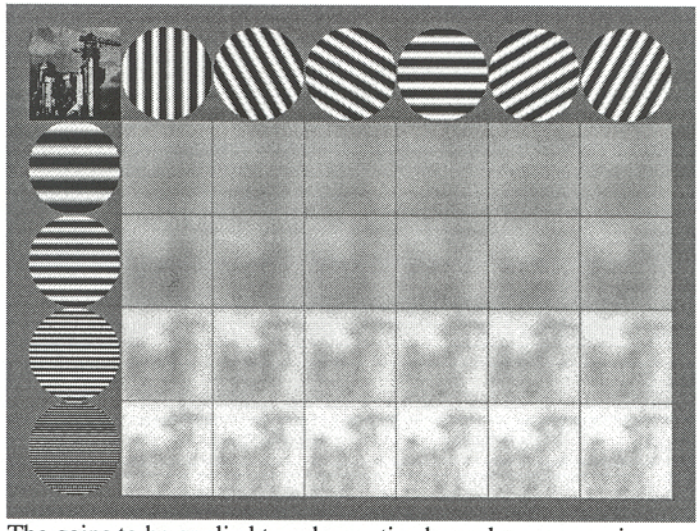

Figure 5. The gains to be applied to achromatic channel responses, in response to the space shuttle image. Higher values indicate higher gains.

The receptive field model that is suggested by the results has two components. First is the standard linear receptive field, which is selective for stimulus spatial frequency, orientation and color properties (e.g., Lennie, Krauskopf and Sclar 1990). These receptive fields determine the immediate response $r(\mathbf{x})$ of the channel. The second component is a large inhibitory surround, somewhat but by no means completely matched to the properties of the center, which has a Gaussian profile, within which contrast is pooled. Activity within this inhibitory surround determines channel gain $g(\mathbf{x})$, which determines the attenuated channel response $g(\mathbf{x}) \times r(\mathbf{x})$. One may place a temporal filter in the pathway that computes local contrast to incorporate the temporal frequency sensitivity and phase lag results of Singer and D'Zmura (1994).

## 3. Discussion

Contrast gain control processing equalizes contrast levels across space (as in Fig. 1) In addition, the center-surround structure of receptive fields leads to a variety of visual illusions with contrast-modulated stimuli. These illusions are analogous to classical visual illusions that depend on lateral inhibition and include second-order Chevreul stripe, Mach band and Craik-O'Brien-Cornsweet stimuli.

The contrast gain control also equalizes contrast levels across spatial frequency and orientation, as illustrated in Figure 6. The image sequence at top results from the repeated application of the contrast gain control model to the space shuttle input image. Below are shown the differences between an output image and the previous image. The first difference, shown in column two, is that between the original image and the immediate output of the contrast gain control, and it shows clearly the spatial equalization of contrast. Contrast is reduced strongly in areas of high contrast, like the shuttle and the rocket, but is little affected in areas of low contrast, like the sky.

ESANN'1997 proceedings - European Symposium on Artificial Neural Networks
Bruges (Belgium), 16-17-18 April 1997, D-Facto public., ISBN 2-9600049-7-3, pp. 67-72

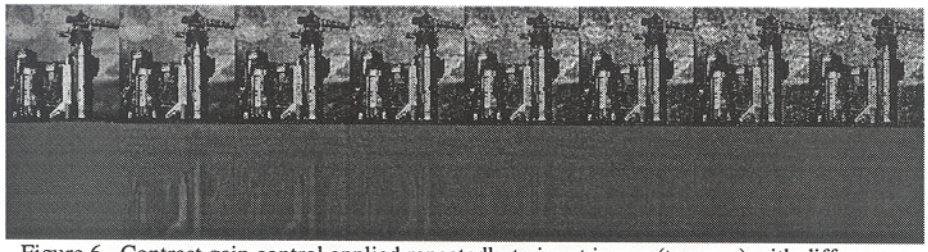

Figure 6. Contrast gain control applied repeatedly to input image (top row) with differences between adjacent members of the sequence shown immediately below (bottom row). The sequence converges on a characteristic image.

Repeated application of the model leads to an image that is not changed by the contrast gain control: the differences fall off to zero. Such an image is a stable point of convergence that characterizes model processing, and it reveals increased energy at orientations and spatial frequencies not present in the original image. Energy is now spread more equally throughout all spatial frequency and orientation bands.

## References

Chubb, C., Sperling, G. and Solomon, J.A. 1989. Texture interactions determine perceived contrast. *Proceedings of the National Academy of Sciences of the United States of America* **86**: 9631-9635.

Derrington, A. M., Krauskopf, J. and Lennie, P. 1984. Chromatic mechanisms in lateral geniculate nucleus of macaque. *Journal of Physiology (London)* **357**: 241-265.

D'Zmura, M. in press. Color contrast gain control. In *Color Vision*, eds. W. Backhaus, R. Kliegl and J. Werner. Berlin: Walter de Gruyter.

D'Zmura, M. and Singer, B. 1996. The spatial pooling of contrast in contrast gain control. *Journal of the Optical Society of America A* **13**: 2135-2140.

Heeger, D.J. 1992. Normalization of cell responses in cat striate cortex. *Visual Neuroscience* **9**: 181-197.

Lennie, P. , Krauskopf, J. and Sclar, G. 1990. Chromatic mechanisms in striate cortex of macaque. *Journal of Neuroscience* **10**: 649-669.

Robson, J.G. 1988. Linear and non-linear operations in the visual system. *Investigative Ophthalmology and Visual Science* **29** *Supplement*: 117.

Shapley, R.M. and Victor, J.D. 1979. The contrast gain control of the cat retina. *Vision Research* **19**: 431-434.

Singer, B. and D'Zmura, M. 1994. Color contrast induction. *Vision Research* **34**: 3111-3126.

Singer, B. and D'Zmura, M. 1995. Contrast gain control: a bilinear model for chromatic selectivity. *Journal of the Optical Society of America A* **12**: 667-685.

Solomon, J.A., Sperling, G. and Chubb, C. 1993. The lateral inhibition of perceived contrast is indifferent to on-center/off-center segregation, but specific to orientation. *Vision Research* **33**: 2671-2683.

Sperling, G. 1989. Three stages and two systems of visual processing. *Spatial Vision* **4**: 183-207.